Journal of Solid State Chemistry 181 (2008) 1909–1914

Contents lists available at ScienceDirect

Journal of Solid State Chemistry

journal homepage: www.elsevier.com/locate/jssc

# Gallium substitutions as a means to stabilize alkaline-earth and rare-earth metal pnictides with the cubic $Th_3P_4$ type: Synthesis and structure of $A_7Ga_2Sb_6$ ($A$ = Sr, Ba, Eu)

Sheng-Qing Xia, Jonathan Hullmann, Svilen Bobev *

*Department of Chemistry and Biochemistry, University of Delaware, Newark, DE 19716, USA*

ARTICLE INFO

*Article history:*
Received 29 February 2008
Received in revised form
28 March 2008
Accepted 3 April 2008
Available online 16 April 2008

*Keywords:*
Zintl phases
Crystal structure
Ga flux

ABSTRACT

Three new compounds—$Sr_{7.04(2)}Ga_{1.94(2)}Sb_6$, $Ba_{7.02(3)}Ga_{1.98(3)}Sb_6$ and $Eu_{7.04(3)}Ga_{1.90(3)}Sb_6$—have been synthesized from reactions of the corresponding elements using gallium as a metal flux. Their crystal structures (space group $I\bar{4}3d$ (No. 220), $Z = 2$ with unit cell parameters: $a = 9.9147(9)$ Å for the Sr-compound; $a = 10.3190(9)$ Å for the Ba-compound; and $a = 9.7866(8)$ Å for the Eu-compound) have been established by single-crystal X-ray diffraction. The structures are best described as Ga-stabilized derivatives of the hypothetical $Sr_4Sb_3$, $Ba_4Sb_3$ and $Eu_4Sb_3$ phases with the cubic $Th_3P_4$ type. Such an inclusion of interstitial Ga atoms in this atomic arrangement results in the formation of isolated $[Ga_2Sb_6]^{14-}$ fragments, isoelectronic and isostructural with the $[Sn_2Te_6]^{6-}$ anions in the $K_3SnTe_3$ type, and allows for the attainment of a charge-balanced electron count. In that sense, the $Sr_4Sb_3$, $Ba_4Sb_3$ and $Eu_4Sb_3$ binaries, which are expected to be electron-deficient and are currently unknown, can be "turned" into $Sr_7Ga_2Sb_6$, $Ba_7Ga_2Sb_6$ and $Eu_7Ga_2Sb_6$, whose structures are readily rationalized following the Zintl concept.



## 1. Introduction

Binary intermetallic compounds crystallizing in the cubic $Th_3P_4$ type (or rather anti-$Th_3P_4$ type) are well known among the rare-earth metal pnictides [1]. The attention of the condensed matter community has long been focused on these phases due to their interesting magnetic and electronic properties [2–7], including Kondo-type behavior [6], valence fluctuations or mixed valence [7]. In contrast, the anti-$Th_3P_4$-type pnictides containing the alkaline-earth metals (or the nominally divalent Eu) are relatively less known and seldom reported. Up until recently, only a few such compounds have been structurally characterized: $Eu_4Bi_3$ [2], $Ba_4P_{2.67}$ [8] and $Ba_8As_5Au$ [9]. In 2003, Corbett and co-workers reported the crystal and electronic structures of $Ba_4Bi_3$, $Sr_4Bi_3$ and $Ba_4As_{2.60}$ [10]. Notably, both bismuthides of this series were shown to be stoichiometric, like $Eu_4Bi_3$ [2]; however, for the lighter P and As, the structures are usually reported to be sub-stoichiometric with respect to the pnicogens (e.g., $Ba_4As_{2.60}$ [10] and $Ba_4P_{2.67}$, the latter also being referred to as $Ba_3P_2$ [8]). The result of this is that the bismuthides are, at least formally, one-electron-deficient whereas the defect phosphides and arsenides are electron-precise Zintl phases. Corbett rationalized these facts by noting that the lighter P and As anions tend to be stabilized as closed-shell species, i.e., taking up three electrons in their valence shells, whereas the very heavy Bi is likely to favor for an open shell configuration [10]. The latter are quite common for the heavy main group elements and are well understood from a theoretical point of view [11]. Comparisons between the structures of $Ba_4Pn_{3-\delta}$ ($Pn$ = P, As, Sb, Bi) could provide very interesting insights into these nuances of the bonding, particularly in the antimony compounds. However, the existence of such binary antimonides of Sr, Ba or Eu has not been reported thus far [1].

With this paper, we report on the synthesis and the characterization of the new compounds, $Sr_{7.04(2)}Ga_{1.94(2)}Sb_6$, $Ba_{7.02(3)}Ga_{1.98(3)}Sb_6$ and $Eu_{7.04(3)}Ga_{1.90(3)}Sb_6$, which perhaps are the closest possible to the antimonides with anti-$Th_3P_4$ structure type [12]. These compounds, hereafter denoted for simplicity as $Sr_7Ga_2Sb_6$, $Ba_7Ga_2Sb_6$ and $Eu_7Ga_2Sb_6$ were serendipitously obtained from Ga flux reactions. Their structures can be viewed as Ga-stabilized derivatives of the hypothetical $Sr_4Sb_3$, $Ba_4Sb_3$ and $Eu_4Sb_3$ phases. We present the structure refinements from single-crystal X-ray diffraction data and discuss the structure in conjunction with our elaborate synthetic efforts and elemental analyses. The formal electron count and the importance of the Ga interstitials are also discussed in the broader context of the Zintl formalism [13].

* Corresponding author. Fax: +1 302 831 6335.
*E-mail address:* bobev@udel.edu (S. Bobev).

0022-4596/$ - see front matter © 2008 Elsevier Inc. All rights reserved.
doi:10.1016/j.jssc.2008.04.004

## 2. Experimental

### 2.1. Synthesis

All manipulations were carried out inside an argon-filled glove box or under vacuum. The starting materials Sr (Aldrich), Ba (Aldrich), Eu (Ames), Ga (Alfa) and Sb (Alfa), all with purity greater than 99.9% (metal basis), were used as received. Gallium was typically used in large excess and was intended as a flux. The routine flux-synthesis method using alumina crucibles sealed in evacuated fused silica jackets was employed. Further details on flux growing methods can be found elsewhere [14]. The metals were loaded with the ratio Sr (Ba or Eu):Ga:Sb = 1.1:10:1 and the optimized temperature profile was the following: (1) quick heating to 950 °C (at rate of 300°/h), (2) homogenization at 950 °C for 27 h and (3) cooling to 400 °C (rate of 10°/h). At this point, the sealed ampoule was removed from the furnace and the molten Ga decanted. Subsequently, the reactions were brought inside the glove box and opened. The typical products were mixtures of large needle-shaped crystals with silver-metallic luster (hexagonal or C-orthorhombic unit cell, unknown structure [15]) and dark-to-black irregular pieces (title compounds). Efforts to synthesize the title compounds as pure phases were unsuccessful.

During our attempts to maximize the yields of these reactions, several relevant observations were made. First, reaction temperatures around 950–1000 °C and fast cooling rates (on the order of 10–15 °C/h) tend to favor the formation of the title compounds in good yields; however, the quality of the crystals obtained in this way was usually poor and not suitable for single-crystal diffraction work (the unknown hexagonal phases were still present). Second, reducing the reaction temperature or the cooling rate did not improve the overall yield. To the contrary, such reactions afforded another type of side product, $AGa_4$ ($A$ = Sr, Ba or Eu) [16] with the tetragonal $BaAl_4$ type [1].

Attempts to extend the series towards $Ca_7Ga_2Sb_6$ or to synthesize the corresponding Bi-analogs failed. The main products of these reactions were $Ca_{11}Sb_{10}$ and $A_{11}Bi_{10}$ ($A$ = Sr, Ba or Eu) with the $Ho_{11}Ge_{10}$ structure type [1].

### 2.2. X-ray powder diffraction

X-ray powder diffraction patterns were taken at room temperature on a Rigaku MiniFlex powder diffractometer using Ni-filtered Cu $K\alpha$ radiation. The diffractometer was enclosed and operated inside a nitrogen-atmosphere glove box, which allowed for the data acquisition for air- and/or moisture-sensitive samples. The data analysis was carried out using the JADE 6.5 software package. The patterns were used for phase identification only; in all three cases the presence of two reaction products was confirmed. As indicated above, the main phases (≈50%) likely crystallize in a hexagonal crystal system (presumed structure types MoC or $Ce_2Pt_6Ga_{15}$ [1], $a \approx 4.4$–$4.6$ Å; $c \approx 17.2$–$18.1$ Å), but due to the extensive disorder, their structures are not yet established [15]. The title compounds were the second products with estimated yields of 30–40%. According to the diffraction data, finely ground powders of $Sr_7Ga_2Sb_6$, $Ba_7Ga_2Sb_6$ and $Eu_7Ga_2Sb_6$ are unstable in air and decompose within minutes. Single crystals also deteriorate quickly, with $Eu_7Ga_2Sb_6$ being the most stable.

### 2.3. Single-crystal X-ray diffraction

Single crystals of the title compounds were picked inside the glove box and cut into suitable sizes for data collection (Table 1). The crystals were mounted on glass fibers using ParatoneN oil and quickly transferred to the goniometer of a Bruker SMART CCD-based diffractometer. To help protect the crystals from decomposition, the crystals were kept under a cold nitrogen gas stream (operating temperature −153 °C). Intensity data were collected in batch runs at three different $\omega$ and $\theta$ angles, covering a full sphere. Frame width was 0.4° and the data acquisition rate was 12 s/frame. Data collection was done with the SMART-software; data integration and global unit cell refinement were carried out using the SAINTplus program [17], respectively ($T_{min}/T_{max} = 0.572$ and $R_{int} = 0.0512$ for $Sr_7Ga_2Sb_6$; $T_{min}/T_{max} = 0.852$ and $R_{int} = 0.0490$ for $Ba_7Ga_2Sb_6$ and $T_{min}/T_{max} = 0.778$ and $R_{int} = 0.0464$ for $Eu_7Ga_2Sb_6$). SADABS was used for semi-empirical absorption correction based on equivalent reflections [18]. The structures were solved by direct methods and refined by full matrix least-squares methods on $F^2$ using SHELX [19]. Further details of the data collection and structure refinement parameters are given in Table 1. Final positional and equivalent isotropic displacement parameters and important bond distances are listed in Tables 2 and 3, respectively. Further information in the form of CIF has been deposited with Fachinformationszentrum Karlsruhe, 76344 Eggenstein-Leopoldshafen, Germany, (fax: (+49) 7247-808-666; e-mail: crysdata@ fiz.karlsruhe.de)—depository number CSD 419226 for $Sr_7Ga_2Sb_6$, CSD 419227 for $Ba_7Ga_2Sb_6$ and CSD 419228 for $Eu_7Ga_2Sb_6$.

**Table 1**
Selected crystallographic data for $A_7Ga_2Sb_6$ ($A$ = Sr, Ba, Eu)

| | | | |
|---|---|---|---|
| Chemical formula | $Sr_{7.04(2)}Ga_{1.94(2)}Sb_6$ | $Ba_{7.02(3)}Ga_{1.98(3)}Sb_6$ | $Eu_{7.04(3)}Ga_{1.90(3)}Sb_6$ |
| Formula weight | 1481.72 | 1831.64 | 1933.88 |
| Space group, $Z$ | | $I\bar{4}3d$ (No. 220), 2 | |
| Unit cell parameters | $a = 9.9147(9)$ Å | $a = 10.3190(9)$ Å | $a = 9.7866(8)$ Å |
| | $V = 974.63(15)$ | $V = 1098.79(17)$ | $V = 937.34(13)$ |
| Radiation, $\lambda$ (Å) | | Mo $K\alpha$, 0.71073 | |
| Temperature, $T$ (K) | | 120(2) | |
| $\theta$ Range for data collection (deg) | 5.04–26.96 | 4.84–27.02 | 5.10–27.16 |
| Crystal size (mm) | 0.06 × 0.05 × 0.03 | 0.06 × 0.05 × 0.05 | 0.06 × 0.05 × 0.03 |
| Data/parameters | 181/11 | 206/11 | 180/11 |
| $\rho_{calcd}$ (g/cm$^3$) | 5.049 | 5.536 | 6.852 |
| $\mu$ (cm$^{-1}$) | 298.21 | 219.24 | 343.07 |
| Absorption correction method | | Semi-empirical (based on equivalents) | |
| Flack parameter | 0.04(2) | 0.09(1) | 0.01(5) |
| Goodness of fit on $F^2$ | 1.303 | 1.202 | 1.128 |
| Final $R_1$ ($I > 2\sigma_I$)[a] | 0.0196 | 0.0222 | 0.0172 |
| Final w$R_2$ ($I > 2\sigma_I$)[b] | 0.0389 | 0.0484 | 0.0398 |

[a] $R_1 = \sum||F_o|-|F_c||/\sum|F_o|$.
[b] $wR_2 = [\sum[w(F_o^2-F_c^2)^2]/\sum[w(F_o^2)^2]]^{1/2}$.

**Table 2**
Atomic coordinates[a] and equivalent ISOTROPIC displacement parameters ($U_{eq}$)[b] for $A_7Ga_2Sb_6$ ($A$ = Sr, Ba, Eu)

| Atom | Site | $x$ | $y$ | $z$ | $U_{eq}$ (Å$^2$) | Occup. |
|---|---|---|---|---|---|---|
| $Sr_7Ga_2Sb_6$ | | | | | | |
| Sr | 16*c* | 0.07416(8) | *x* | *x* | 0.0333(4) | 0.876(3) |
| Sb | 12*a* | 3/8 | 0 | 1/4 | 0.0279(2) | 1.0 |
| Ga1 | 16*c* | 0.0099(5) | *x* | *x* | 0.020(2) | 0.124(3) |
| Ga2 | 16*c* | 0.1559(5) | *x* | *x* | 0.020(2) | 0.124(3) |
| $Ba_7Ga_2Sb_6$ | | | | | | |
| Ba | 16*c* | 0.92622(7) | *x* | *x* | 0.0327(3) | 0.877(4) |
| Sb | 12*a* | 5/8 | 0 | 3/4 | 0.0320(4) | 1.0 |
| Ga1 | 16*c* | 0.9893(7) | *x* | *x* | 0.019(3) | 0.123(4) |
| Ga2 | 16*c* | 0.8446(7) | *x* | *x* | 0.019(3) | 0.123(4) |
| $Eu_7Ga_2Sb_6$ | | | | | | |
| Eu | 16*c* | 0.92523(6) | *x* | *x* | 0.0283(3) | 0.880(4) |
| Sb | 12*a* | 5/8 | 0 | 3/4 | 0.0222(3) | 1.0 |
| Ga1 | 16*c* | 0.9906(7) | *x* | *x* | 0.016(2) | 0.120(4) |
| Ga2 | 16*c* | 0.8443(7) | *x* | *x* | 0.016(2) | 0.120(4) |

[a] The reported coordinates are in different settings because in order to obtain the correct absolute structure in the refinements, the coordinates had to be inverted.
[b] $U_{eq}$ is defined as 1/3 of the trace of the orthogonalized $U_{ij}$ tensor.

**Table 3**
Important bond distances $A_7Ga_2Sb_6$ ($A$ = Sr, Ba, Eu)

| Atom pair | | Distance (Å) | Atom pair | | Distance (Å) |
|---|---|---|---|---|---|
| $Sr_7Ga_2Sb_6$ | | | | | |
| Ga1 | 3 × Sb | 2.820(3) | Sr | 3 × Sb | 3.3353(9) |
| | Ga2 | 2.508(12) | | 3 × Sb | 3.5323(9) |
| Ga2 | 3 × Sb | 2.824(3) | | Ga1 | 3.190(8) |
| | Ga1 | 2.508(12) | | Ga2 | 2.889(8) |
| $Ba_7Ga_2Sb_6$ | | | | | |
| Ga1 | 3 × Sb | 2.940(4) | Ba | 3 × Sb | 3.4673(8) |
| | Ga2 | 2.585(16) | | 3 × Sb | 3.6807(9) |
| Ga2 | 3 × Sb | 2.943(4) | | Ga1 | 3.341(13) |
| | Ga2 | 2.585(16) | | Ga2 | 3.010(12) |
| $Eu_7Ga_2Sb_6$ | | | | | |
| Ga1 | 3 × Sb | 2.781(4) | Eu | 3 × Sb | 3.2984(7) |
| | Ga2 | 2.481(15) | | 3 × Sb | 3.4799(7) |
| Ga2 | 3 × Sb | 2.789(4) | | Ga1 | 3.129(12) |
| | Ga2 | 2.481(15) | | Ga2 | 2.866(11) |

We note here that the refinement cycles using the coordinates from the stoichiometric phase $Ba_4Bi_3$ as a model [10], immediately indicated a problem with it—the *R*-values were higher than 10–15% and a significant electron density was left unaccounted for. Subsequent refinements with freed occupation factors suggested that in all three structures the Sb atoms are fully occupied while the cations refine as ca. 88% occupied. This led to modest improvements of the final residuals, but the two peaks in the difference Fourier map (greater than 6–8 e$^-$/Å$^3$, less than 1.5 Å from away from the cation position) persisted. When Sb atoms were assigned at those positions and refined with fractional occupancies, the refinements improved, but the occupation factors were lower than 6–7%. Furthermore, the structural model lacked a physical meaning. At this point, the possibility for Ga inclusions (from the flux) was recognized and tested. The two partially occupied positions were refined as Ga atoms, which resulted in an occupancy factor of nearly 12%—note that the occupancies of the two independent Ga sites refined almost the same (within 3$\sigma$). The interpretation of this model is straightforward—the 12% occupancy for the gallium atoms is complimentary to the 88% occupancy of the nearby cation; thus, when the cation residing in the Sb-octahedron is missing in a random manner, the vacant position is taken up by a dimer of Ga atoms. Such substitution will yield isolated $[Ga_2Sb_6]^{14-}$ species, isosteric with the $Si_2Cl_6$ molecule. The final refinements for all three compounds converged readily to very low residuals and were consistent with the elemental microanalysis described below.

### 2.4. EDX analysis

Elemental analysis and confirmation of the composition obtained from structure refinements was possible only for the crystals of $Eu_7Ga_2Sb_6$. As mentioned above, this was the only compound that could be handled in ambient atmosphere (only for a very short period of time). Single crystals of $Eu_7Ga_2Sb_6$ were selected under a microscope in the glove box and mounted onto carbon tape. The specimen was then transferred to the vacuum chamber of a Jeol 7400 F electron microscope, equipped with an INCA-Oxford energy-dispersive spectrometer. The microscope was operated at 10 μA beam current and a 15 kV accelerating potential. Several crystals were analyzed and the average ratio of the elements normalized per Sb (atomic %) was Eu:Ga:Sb = 6.4:2.1:6. This is consistent with the refined ratio of Eu:Ga:Sb = 7:2:6.

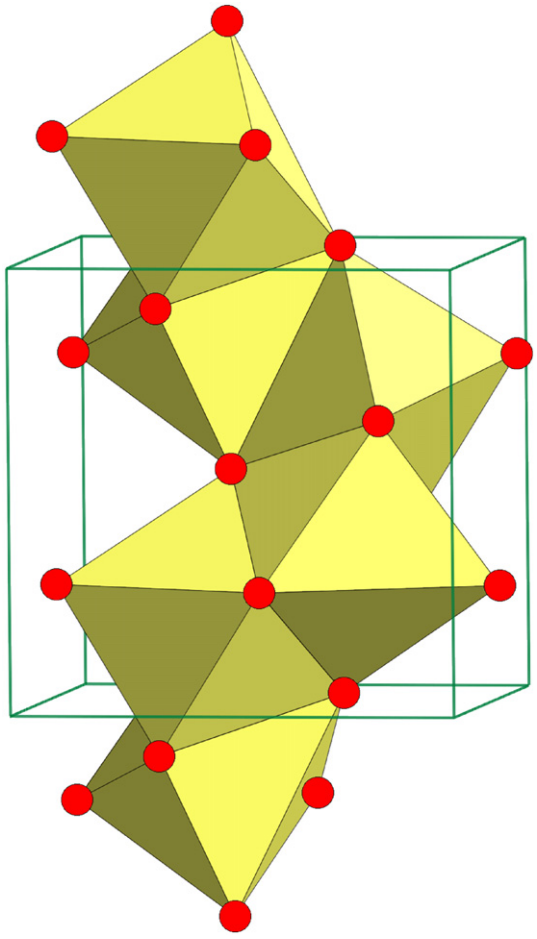

**Fig. 1.** A polyhedral representation of the structure of the hypothetical $Sr_4Sb_3$, $Ba_4Sb_3$ and $Eu_4Sb_3$ phases with the body-centered cubic anti-$Th_3P_4$ type. The $Sr^{2+}$, $Ba^{2+}$ or $Eu^{2+}$ cations (not shown for clarity) reside inside the distorted octahedra of antimony $Sb^{3-}$ anions. The acentric way of packing of these octahedra is emphasized.

### 2.5. Magnetic susceptibility measurements

Magnetization ($M$) as a function of the temperature was measured on a Quantum Design MPMS SQUID magnetometer for a polycrystalline $Eu_7Ga_2Sb_6$. The sample (5 mg) was prepared in the glove box by carefully selecting crystals under a microscope and loading them into a specially designed holder for air-sensitive materials [20]. Measurements were done in the temperature interval 5–290 K in an applied field ($H$) of 1000 Oe (field cooling mode). The holder's diamagnetic contribution to the magnetization was subtracted when the raw data were converted to molar susceptibility ($\chi_m = M/H$). For convenience the data were normalized per mol Eu, not per formula unit.

## 3. Results

### 3.1. Structure description

The structures of $Sr_7Ga_2Sb_6$, $Ba_7Ga_2Sb_6$ and $Eu_7Ga_2Sb_6$, at least formally, are substitutional derivatives of the body-centered cubic $Th_3P_4$ type [1]. Since the general description and some specific details of this common structure type (Fig. 1) have been discussed in earlier reports [2,10], here we will only focus our attention on the unique features of the new phases in conjunction with the role of the Ga interstitials as it pertains to the stabilization of structure.

To better illustrate the topological relationship between $A_4Sb_3$ (the inverse of the $Th_3P_4$ type) and $A_7Ga_2Sb_6$, we re-write their formulas as $A_8Sb_6$ and $A_{8-x}Ga_{2x}Sb_6$ ($A$ = Sr, Ba, Eu), respectively. The structure of the hypothetical binary antimonides $A_8Sb_6$ represents an overall complex arrangement of antimony anions and rare-earth or alkaline-earth metal cations with otherwise simple local coordination. As illustrated in Fig. 1, the cations are located at the centers of distorted octahedra of antimony anions. They, in turn, are coordinated by eight cations. There are no anion–anion contacts. Note that the Sr, Ba or Eu cations take the P site (Wyckoff index 16*c*) and the Sb anions occupy the Th sites (Wyckoff index 12*a*).

The structure of the new ternary $A_{8-x}Ga_{2x}Sb_6$ compounds can be derived from the structure of $A_8Sb_6$ by substituting one of every eight cations (i.e., $x = 1$) with a pair of Ga atoms. If such an exchange is done in a periodic fashion, it is reasonable to expect an ordered "super-structure" to be realized; however, we find no evidence for a long-range order as the substitutions appear to be randomly distributed (see Experimental details). In fact, the three compounds we report crystallize in the same space group, $I\bar{4}3d$ (No. 220), as all other $A_8Pn_6$ pnictides ($A$ = Sr, Ba, Eu; $Pn$ = As, Bi) [2,10] and their unit cell parameters are comparable. We also point out that based on the similar crystal chemistry of many Ga and In compounds it can be expected that the $A_{8-x}In_{2x}Sb_6$ analogs may exist and provide further evidence for the random nature of these replacements. Although we attempted to extend our studies in this direction, it appears that In may be too large to fit into the octahedral holes in the structures of these compounds (Fig. 2). The only exception to this is with the largest $Ba^{2+}$ cations [15]. Powder diffraction data and several indexed single crystals confirm the existence of $Ba_7In_2Sb_6$, but satisfactory structure refinements could not be obtained (final residuals are on the order of 10%) and this structure is not discussed. Nonetheless, the refined unit cell constant for this $Ba_{8-x}In_{2x}Sb_6$ phase, $a = 10.476(5)$ Å [21] is intermediate between the unit cell constant for $Ba_{8-x}Ga_{2x}Sb_6$, $a = 10.3190(1)$ Å, and the unit cell constant for the stoichiometric $Ba_8Bi_6$ phase, $a = 10.550(1)$ Å [10], nicely corroborating this model. More definitive evidence for the incorporation of Ga metal in the structure is the excellent agreement between the refined from single-crystal work and the obtained from elemental analysis compositions.

Having confirmed the cation disorder and the inclusion of Ga (or In) in the structure, the question of how to relate the $A_{8-x}Ga_{2x}Sb_6$ structure to some other ternary phases with Ga–Sb polyanionic sub-networks arises. Since the refined occupancies of the cations in the three structures are close to 88%, i.e., 1/8 of the cation sites are actually vacant, it is conceivable that the Ga dimers fill the empty space created by the absent cations. These Ga dimers are formed by two crystallographically independent Ga atoms (Table 2), which are both about 12% occupied. Both Ga sites lie on the three-fold axes and their inclusion generates several short contacts between symmetry equivalent positions. However, due to the very low site-occupancy, only one of approximately eight, these distances are not problematic for the interpretation of the structure and the actual Ga—Ga separation is ca. 2.5 Å (Table 3) [21]. As a consequence, the inclusion of the two Ga atoms in this octahedral atomic arrangement results in the formation of isolated $[Ga_2Sb_6]^{14-}$ fragments, isoelectronic and isostructural with the $[Sn_2Te_6]^{6-}$ anions in the $K_3SnTe_3$ type [22] or their phosphide analogs $[Sn_2P_6]^{12-}$ as seen in the $Ba_6[Sn_2P_6]$ structure [23]. A schematic illustration of such a fragment is presented in Fig. 2. All resultant Ga–Sb distances are very reasonable, ranging from 2.781(4) to 2.943(4) Å. These compare very well with the Ga–Sb distances in other intermetallic compound whose structures are based on similar structural motifs: $Yb_{11}GaSb_9$ [24], isolated $GaSb_4$; $Sr_3GaSb_3$ [25], linear $GaSb_2$ chains; $Ca_5Ga_2Sb_6$ [26], $Ga_2Sb_6$ ribbons; and $Ba_7Ga_4Sb_9$ [27], 3D $Ga_4Sb_9$ network.

### 3.2. Electron count

The analogy with the $K_3SnTe_3$ provides some useful clues as to how the $A_7Ga_2Sb_6$ structures ($A$ = Sr, Ba, Eu) can be rationalized and understood. It is well known that stoichiometric pnictides with the anti-$Th_3P_4$ structure containing divalent cations will be electron-deficient [10]. This is due to the cations providing only eight electrons while the isolated pnicogen anions ($Pn$) require nine electrons to complete their octets as $Pn^{3-}$ [13]. For example, this has been discussed for $Ba_4As_{2.60}$ [10] and $Ba_4P_{2.67}$ [8], which are sub-stoichiometric, but electron-precise Zintl phases. The tendency of the Bi compounds to be defect-free has been explained by taking into account the likelihood of Bi to favor hypervalent bonding, while the lighter P and As anions tend to be stabilized as closed-shell species [10]. No binary "4–3" antimonides of the alkaline-earth or the divalent rare-earth metals are known [28]. This suggests that the hypothetic $Sr_4Sb_3$, $Ba_4Sb_3$ and $Eu_4Sb_3$ phases are likely unstable with respect to the elements or the neighboring $A_{11}Sb_{10}$ phases in the corresponding binary phase diagrams [10]. Furthermore, since the sub-stoichiometric $A_4Sb_{3-\delta}$ compounds are also unknown and our efforts to synthesize such compounds failed we speculate that creating Sb vacancies in these cases is not favored. Nature, obviously, prefers another mechanism for the stabilization of this structure through the inclusion of a more electron poor element, such as Ga or In. In this case, these elements form homoatomic Ga–Ga or In–In bonds. Following the Zintl formalism [13], the replacement of a divalent cation in an octahedral site, formally $[ASb_6]^{16-}$ (denoting the $A^{2+}$ cation at the center of an octahedron of isolated $Sb^{3-}$ anions), with a $[Ga_2Sb_6]^{14-}$ or $[In_2Sb_6]^{14-}$ fragment will lead to a net 2-electron reduction of the overall electron requirement when comparing $A_8Sb_6$ with $A_7Ga_2Sb_6$. Therefore, due to the provision of exactly 14 electrons by the 7 divalent cations, the $A_7Ga_2Sb_6$ ($A$ = Sr, Ba, Eu) phases obey the Zintl rules and should be considered as typical Zintl phases with closed-shell electron configurations for all atoms. In sharp contrast, $A_8Sb_6$ are clearly electron-deficient and

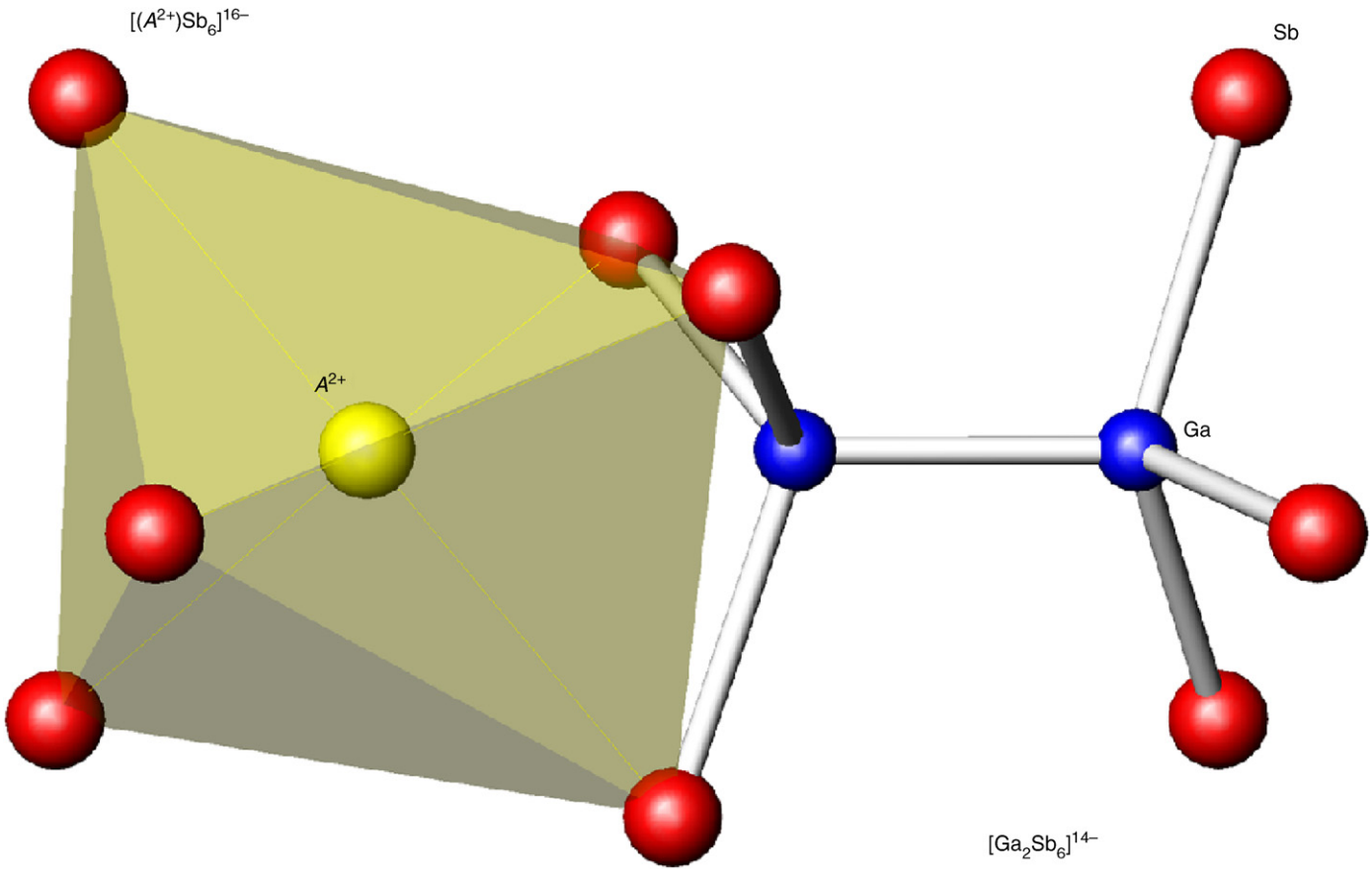


**Fig. 2.** A schematic illustration of the disorder model for $A_7Ga_2Sb_6$ ($A$ = Sr, Ba, Eu). 1/8 of the cation sites in the structure are actually filled with Ga dimers. Their inclusion in the octahedral coordination environment results in the formation of isolated $[Ga_2Sb_6]^{14-}$ fragments, isosteric with $[Sn_2P_6]^{12-}$ anions in the $Ba_6[Sn_2P_6]$ structure. Relevant distances are listed in Table 3.

will be unlikely to form. This conclusion is fully supported by the experimental and theoretical work by Corbett and co-workers, who suggest that $Ba_8Sb_6$ cannot be synthesized, but could, conceivably, be stabilized as $Ba_8Sb_5I$ [10]. This idea has already been exemplified in $Ba_8As_5Au$ [9].

### 3.3. Magnetic susceptibility

The temperature dependence of the dc magnetization of $Eu_7Ga_2Sb_6$ is presented in Fig. 3 (plotted is the magnetic susceptibility $\chi = M/H$ versus $T$). The polycrystalline sample was field cooled from room temperature down to 5 K in increments of 10° to 60 K and smaller thereafter (5° to 15 K and 1° to 5 K). As shown in the inset, the inverse of the susceptibility ($\chi^{-1}$) is linear above ca. 15 K, indicating that $Eu_7Ga_2Sb_6$ is paramagnetic in this temperature range and follows the Currie–Weiss law [29]. The calculated effective moment for Eu is 7.5(1) $\mu_B$. The value, as expected, is consistent with divalent Eu, which has 7 unpaired electrons (theoretically predicted moment according to the Hund's rule, $\mu_{calc} = 7.94\,\mu_B$) [29]. The agreement between the theoretical value and the experimentally determined moment is not perfect. This is probably due to a small amount of an impurity phase present such as the unidentified Eu–Ga–Sb compound with a hexagonal structure (silver needles) which is always co-existing with $Eu_7Ga_2Sb_6$ (black pieces). The two phases were mechanically separated under a microscope but possible contamination cannot be completely ruled out. Below 7 K, the structure undergoes a magnetic phase transition and the Eu spins appear to order

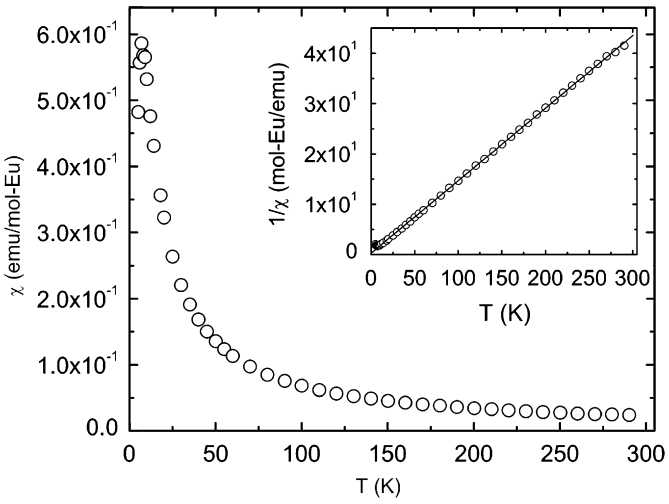


**Fig. 3.** Plot of the magnetic susceptibility ($\chi = M/H$) versus $T$ for $Eu_7Ga_2Sb_6$. Data are collected in a field-cooling mode ($H$ = 1000 Oe) and normalized per mol-Eu. *Inset*: Inverse susceptibility ($\chi^{-1}$) as a function of the temperature. The linear fit to the Curie–Weiss law ($\chi(T) = C/(T-\theta_{CW})$) is also shown.

antiferromagnetically ($T_N = 7$ K; $\theta_{CW} = -2$ K). These results are similar to the magnetic properties of the related $Eu_4Bi_3$ phase, which also orders antiferromagnetically ($T_N = 18$ K) and exhibits divalent europium [2].

## 4. Conclusions

The structures of three new ternary compounds with nominal divalent cations: $Sr_{7.04(2)}Ga_{1.94(2)}Sb_6$, $Ba_{7.02(3)}Ga_{1.98(3)}Sb_6$ and $Eu_{7.04(3)}Ga_{1.90(3)}Sb_6$ have been determined by single-crystal X-ray diffraction. They are best described as Ga-stabilized derivatives of the hypothetical $Sr_4Sb_3$, $Ba_4Sb_3$ and $Eu_4Sb_3$ phases with the body-centered cubic anti-$Th_3P_4$ type. The formal electron count and the importance of the Ga interstitials have also been discussed; unlike the one-electron-deficient $A_4Sb_3$ phases ($A$ = Sr, Ba, Eu), the new ternary compounds are deemed to be Zintl phases with closed-shell configurations for both cations and anions. Current efforts are focused on studying the transport and electronic properties of these compounds as they are expected to be small-gap semiconducting materials. Concurrent efforts are put forth for growing better quality crystals and determining the structures of the new hexagonal phases discovered in the Sr–Ga–Sb, Ba–Ga–Sb and Eu–Ga–Sb ternary systems.

## Acknowledgments

Svilen Bobev gratefully acknowledges funding from the University of Delaware and the Petroleum Research Fund (ACS-PRF). Jonathan Hullmann wishes to thank the organizers of the NSF Summer Research Program in Solid State Chemistry and Materials and the Howard Hughes Medical Institute (HHMI) for the summer research fellowships.

## References

[1] (a) P. Villars, L.D. Calvert, Pearson's Handbook of Crystallographic Data for Intermetallic Phases, second ed, American Society for Metals: Materials Park, OH, 1991;
(b) P. Villars, Pearson's Handbook of Crystallographic data for Intermetallic Phases Desktop Edition, American Society for Metals: Materials Park, OH, 1997.
[2] M.E. Wang, J.T. Chang, S.M. Kauzlarich, Z. Anorg. Allg. Chem. 622 (1996) 432.
[3] V.N. Antonov, B.N. Harmon, A.N. Yaresko, Phys. Rev. B 72 (2005) 085119.
[4] M. Kohgi, K. Iwasa, J.M. Mignot, A. Ochiai, T. Suzuki, Phys. Rev. B 56 (1997) R11388.
[5] M. Kohgi, K. Iwasa, J.M. Mignot, B. Fak, P. Gegenwart, M. Lang, A. Ochiai, H. Aoki, T. Suzuki, Phys. Rev. Lett. 86 (2001) 2439.
[6] (a) A. Ochiai, T. Suzuki, T. Kasuya, J. Magn. Magn. Mater. 52 (1985) 13;
(b) Y.S. Kwon, A. Ochiai, H. Kitazawa, N. Sato, H. Abe, T. Nanba, M. Ikezawa, K. Takegahara, O. Sakai, T. Suzuki, T. Kasuya, J. Magn. Magn. Mater. 70 (1987) 397;
(c) J.A. Alonso, J.X. Boucherle, J. Rossat-Mignod, J. Schweizer, J. Magn. Magn. Mater. 103 (1992) 179.
[7] (a) H. Aoki, A. Ochiai, T. Suzuki, R. Helfrich, F. Steglich, Physica B 230-232 (1997) 698;
(b) G. Borzone, R. Ferro, N. Parodi, A. Saccone, Gazz. Chim. Ital. 125 (1995) 263;
(c) A. Ochiai, D.X. Li, Y. Haga, O. Nakamura, T. Suzuki, Physica B 188 (1993) 437;
(d) A. Ochiai, S. Nakai, A. Oyamada, T. Suzuki, T. Kasuya, J. Magn. Magn. Mater. 47&48 (1985) 570.
[8] (a) K.E. Maass, Z. Anorg. Allg. Chem. 374 (1970) 11;
(b) C. Hadenfeldt, H.-U. Terschüren, W. Hönle, L. Schröder, H.G. Von Schnering, Z. Anorg. Allg. Chem. 619 (1993) 843.
[9] J. Nuss, M. Jansen, Z. Kristallogr. New Cryst. Struct. (NCS) 217 (2002) 313.
[10] B. Li, A.-V. Mudring, J.D. Corbett, Inorg. Chem. 42 (2003) 6940.
[11] (a) G. Papoian, R. Hoffmann, Angew. Chem. Int. Ed. 39 (2000) 2409;
(b) M.L. Munzarova, R. Hoffmann, J. Am. Chem. Soc. 124 (2002) 4787;
(c) G. Papoian, R. Hoffmann, J. Am. Chem. Soc. 123 (2001) 6600;
(d) A. Ienco, R. Hoffmann, G. Papoian, J. Am. Chem. Soc. 123 (2001) 2317.
[12] $Sr_4As_3$ and $Ba_4P_3$ are known "4–3" pnictides (M. Somer, W. Carrillo-Cabrera, K. Peters, H.G. von Schnering, Z. Kristallogr. 210 (1995) 876); however their structures are very different from the ones discussed in this paper.
[13] (a) E. Zintl, Angew. Chem. 52 (1939) 1;
(b) R. Nesper, Prog. Solid State Chem. 20 (1990) 1;
(c) S.M. Kauzlarich (Ed.), Chemistry, Structure, and Bonding of Zintl Phases and Ions, VCH Publishers, New York, 1996.
[14] (a) P.C. Canfield, Z. Fisk, Philos. Mag. B 65 (1992) 1117;
(b) M.G. Kanatzidis, R. Pöttgen, W. Jeitschko, Angew. Chem. Int. Ed. Engl. 44 (2005) 6996.
[15] S.-Q. Xia, J. Hullmann, S. Bobev, unpublished results.
[16] (a) P.H. Tobash, Y. Yamasaki, S. Bobev, Acta Crystallogr. E 61 (2005) 1174;
(b) S. Bobev, E.D. Bauer, J.D. Thompson, J.L. Sarrao, J. Magn. Magn. Mater. 277 (2004) 236;
(c) G. Bruzzone, Acta Crystallogr. 18 (1965) 1081.
[17] Bruker SMART and SAINT, Bruker AXS Inc., Madison, WI, USA, 2002.
[18] G.M. Sheldrick, SADABS, University of Göttingen, Germany, 2003.
[19] G.M. Sheldrick, SHELXTL, University of Göttingen, Germany, 2001.
[20] S.-Q. Xia, S. Bobev, Inorg. Chem. 46 (2007) 874.
[21] $Ba_7In_2Sb_6$ in $I\bar{4}3d$ (No. 220), 2; $a = 10.476(5)$ Å, $V = 1149.7(3)$ Å. The refined In–Sb and In–In distances are 2.962(9) Å and 2.79(1) Å, respectively.
[22] G. Dittmar, Z. Anorg. Allg. Chem. 453 (1979) 68.
[23] B. Eisenmann, H. Jordan, H. Schäfer, Z. Naturforsch. 38B (1983) 404.
[24] S. Bobev, V. Fritsch, J.D. Thompson, J.L. Sarrao, B. Eck, R. Dronskowski, S.M. Kauzlarich, J. Solid State Chem. 178 (2005) 1071.
[25] G. Cordier, H. Schäfer, M. Stelter, Z. Naturforsch. 42B (1987) 1268.
[26] G. Cordier, H. Schäfer, M. Stelter, Z. Naturforsch. 40B (1985) 5.
[27] G. Cordier, H. Schäfer, M. Stelter, Z. Anorg. Allg. Chem. 534 (1986) 137.
[28] $Yb_4Sb_3$ is known, but it is actually a mixed-valent compound (ref. 7d), not electron-deficient like the remaining $A_4Sb_3$ with divalent $A^{2+}$ cations.
[29] C. Kittel, Introduction to Solid-State Physics, seventh ed, Wiley, 1996.